Quantum Electronics **48** (10) 977–982 (2018)

LASER PHOTOEMISSION

https://doi.org/10.1070/QEL16754

Surface localisation of laser photoelectron emission using Cu_2O and Ag film structures

S.V. Andreev, P.A. Danilov, S.I. Kudryashov, E.A. Ryabov

Abstract. **A laser electron source localised on a photocathode surface was developed on the basis of Ag and Cu_2O thin films sequentially deposited by magnetron sputtering on a glass substrate. Photoemission of electrons under the action of the fourth (263 nm) harmonic of a femtosecond fibre laser was initiated from the surface of an Ag film deposited on the substrate surface. Photoelectron source localisation on the photocathode surface was provided by sputtering the Cu_2O copper oxide film on its surface, which significantly (about 50 times) reduced the photoemission efficiency, and by subsequent removal of the copper oxide layer in the photoemission spot with a diameter of ~15 μm by means of focused second-harmonic radiation of a femtosecond fibre laser. In conducting research on the photocathode surface, a grid of photoemission spots was formed, which greatly facilitated the laser beam alignment with the photoemission spot. A decrease in the noises of ultrafast transmission electron microscope, associated with spatial fluctuations of the laser beam initiating pulsed photoelectron emission from the microscope photocathode when using a localised electron source on the basis of a structure of thin Cu_2O and Ag films, was experimentally demonstrated.**

Keywords: *laser photoelectron emission, localised source of photoelectrons, ultrafast electron microscope.*

1. Introduction

The process of electron emission under the action of radiation is one of the most studied physical phenomena. Based on these studies, various photocathodes have been developed for engineering applications. As the main criteria for assessing the quality of photocathodes, the efficiency of electron emission from a photocathode, its radiation resistance, and the spatial stability of photoemission are usually considered. The latter factor becomes especially important when the photoemission process is used to form electron beams to study physical processes that manifest themselves in beam deflection. In these studies, spatial fluctuations of the electron beam may lead to large noises in the measurements. This situation occurs, for example, when a thermionic cathode is replaced by a photocathode in an ultrafast electron microscope or electron diffractometer to operate in the dynamic regime [1–4]. In these devices, spatial fluctuations in the electron beam formed as a result of photoemission may lead to the fluctuations of the image or diffraction pattern (in the case of electron diffractometer) produced by such a beam, which in turn leads to additional noises in the measurements.

When using traditional surface photocathodes with a photoemission layer deposited on a planar surface, the area of which is much larger than the spot area of laser radiation initiating the emission of electrons, spatial fluctuations of the laser beam can largely contribute to the spatial instability of the electron beam. The effect of these fluctuations becomes especially noticeable when the laser source and the device that uses this source to trigger photoemission from the cathode are located at a considerable distance from each other and may be subjected to asynchronous mechanical vibrations.

Currently, another type of photocathodes, so-called tip photocathodes, is widely used [5–8]. When using these photocathodes, photoemission of electrons under the action of laser radiation is performed from the surface of a tip, the size of which may constitute about several tens of nanometers. This makes it possible to develop a tip-based localised source of photoelectrons and form an electron beam with high spatial performance.

Along with high performance, tip photocathodes have significant disadvantages such as the complexity of manufacturing and low efficiency of the laser radiation use, which are due to their small photoemission surface compared to the laser beam diameter. Besides, these photocathodes are inferior to conventional flat photocathodes in such important parameters as versatility and mechanical stability.

In this regard, it is of interest to develop methods to improve the performance of flat photocathodes, in particular, to increase the spatial stability of electron beams being formed with the use of such photocathodes in the presence of spatial fluctuations of laser radiation initiating photoemission.

One of the possible ways to reduce the spatial fluctuations of electron beams emitted from the photocathode surface is to limit the electron emission region and to form localised areas on its surface, i.e. spots or points of photoemission. The localisation of photoemission makes it possible to reduce the spatial fluctuations of the electron beam emitted from the photocathode surface in the presence of laser radiation fluctuations.

It should be noted that the impact of limiting the photoemission region on the photoelectron beam stability was observed in [9] by using a LaB_6 'pin' cathode with a diameter of 50–100 μm, surrounded by a protective graphite ring.

This paper proposes a method for photoemission localisation on the surface of a conventional thin-film metal photo-

S.V. Andreev, E.A. Ryabov Institute for Spectroscopy, Russian Academy of Sciences, ul. Fizicheskaya 5, Troitsk, 108840 Moscow, Russia; e-mail: fcenter@isan.troitsk.ru;
P.A. Danilov, S.I. Kudryashov P.N. Lebedev Physical Institute, Russian Academy of Sciences, Leninsky prosp. 53, 119991 Moscow, Russia; e-mail: Pavel-Danilov2009@yandex.ru

Received 19 June 2018; revision received 31 July 2018
Kvantovaya Elektronika **48** (10) 977–982 (2018)
Translated by M.A. Monastyrskiy

cathode, which consists in depositing of a thin Cu_2O copper oxide film with low photoemission efficiency on its surface, followed by removal of this film in the photoemission spot. The Cu_2O film in the spot was removed by focused radiation from a femtosecond fibre laser.

2. Experiment

The structure of the sample used as a photocathode in the experiment is shown in Fig. 1. The sample was a thin glass substrate with a thickness of 160 μm and a size of about 8 × 8 mm, cut from a standard cover plate used in an optical microscope. An Ag film with a thickness of ~100 nm, used as photoemission material, and a Cu_2O film, which, due to its high work function of electrons (about 4.84 eV) [10], has a low photoemission efficiency under the action of radiation quanta used in the experiment (4.72 eV), were sequentially deposited on the substrate by the method of magnetron sputtering. The Cu_2O film was formed as a result of copper oxidation in the process of copper target sputtering in the Ar atmosphere containing an admixture of oxygen. The technique of Cu_2O film deposition and the film characteristics are presented in detail in [11].

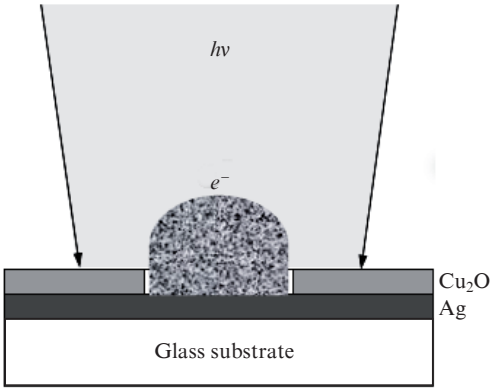

Figure 1. Sample structure used as a photocathode.

The deposition of a thick enough copper oxide film preventing the emission of electrons from the sample reduced significantly (about 50 times) the efficiency of photoemission from the Cu_2O–Ag structure compared to the Ag film. The Cu_2O film thickness was selected experimentally and constituted ~150 nm.

To initiate photoemission at a given location on the Cu_2O–Ag structure surface, a copper oxide layer was removed to the level of Ag photoemission layer (see Fig. 1). The removal of the Cu_2O layer in the photoemission spot was performed on an experimental stand for micro- and nanostructuring [12] using the second-harmonic radiation from a Satsuma femtosecond fibre laser (Amplitude Systems; second harmonic wavelength of 515 nm, FWHM pulse duration of 200 fs, maximum pulse energy of 4 μJ in the TEM_{00} mode, pulse repetition rate f = 0–2 MHz). Laser radiation was focused in the air onto the sample surface through an optical microscope lens with a numerical aperture NA = 0.1. The minimum laser spot radius at the focus was $R_{1/e}$ = 4.4 ± 0.2 μm. To obtain the required photoemission spot diameter, the laser spot diameter on the sample surface was increased by shifting the lens focus position by 300 μm from the sample surface. The laser pulse energy was chosen so as to ensure that the copper oxide layer was removed in a single pulse and the Ag photoemission layer was affected to the minimum possible extent (typical energy value in the experiment was about 1.2 μJ). The sample displacement relative to the laser beam from pulse to pulse was conducted using a three-coordinate motorised stage with a minimum step of 150 nm.

Visualisation of the structure surface relief after irradiation was performed using a JEOL7001F scanning electron microscope (SEM). The SEM image of the resulting photoemission spot is shown in Fig. 2a.

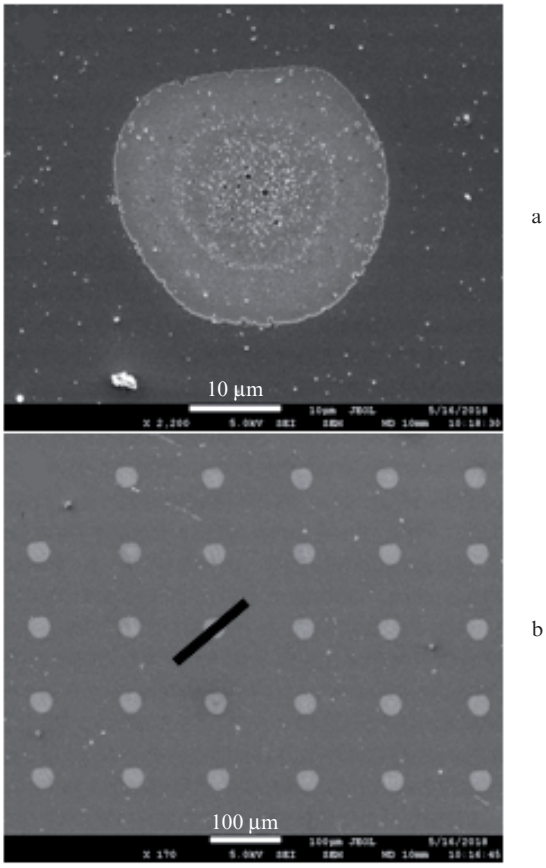

Figure 2. SEM images of (a) the resulting photoemission spot (internal spot is a photoemission spot, external spot is a processing laser spot) and (b) grids of photoemission spots on the structure surface. Dark stripe on the grid of spots shows the scanning range of the laser beam (see the text).

Figure 3a shows an image of the Cu_2O–Ag structure region, obtained using an optical microscope at the location where the copper oxide was removed in order to form a photoemission spot. For comparison, Fig. 3b shows a fragment of an image of a similar sample with a photoemission layer of Ag, but with no Cu_2O film deposited on top. These images were obtained by illumination of samples in transmission regime at the same illumination brightness and microscope magnification. Comparison of both images clearly shows that, in the central part of the spot on the area with a diameter of ~15 μm, the Cu_2O film is absent, and in this part only few small fragments of Cu_2O film are observed (dark spots in Fig. 3a), which, apparently, got there at the laser pulse end.

A deepening on the Cu_2O–Ag structure surface, formed by the above method, served as a source of photoemission,

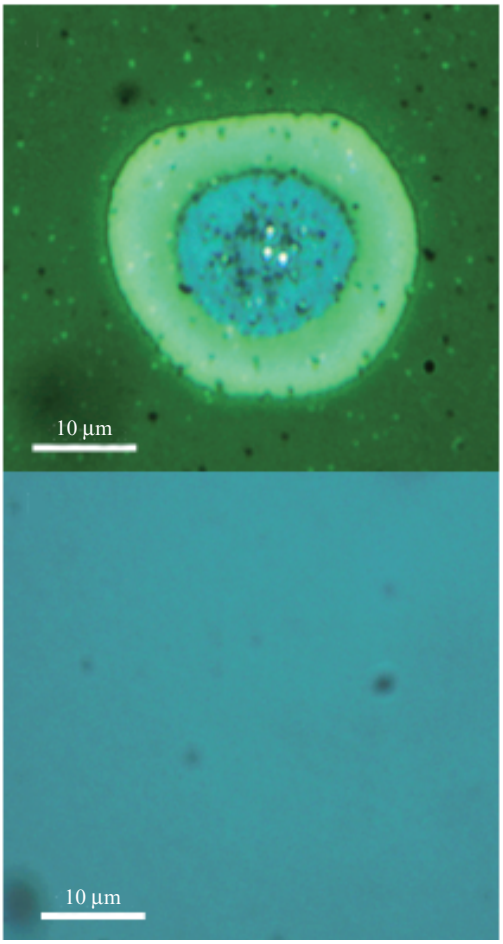

Figure 3. (Colour online) (a) Image of the Cu_2O–Ag structure area, obtained using an optical microscope at the location where copper oxide was removed in order to form a photoemission spot, and (b) fragment of the image of a similar sample with a photoemission layer of Ag, but with no Cu_2O film deposited from above.

assembly (Fig. 4) and fastened to the surface using a pressure ring with a diameter of 8 mm, made of freshly polished copper wire with a diameter of 500 μm. To ensure electrical contact between the cathode assembly and electron-emitting silver layer of the Cu_2O–Ag structure under study, the upper insulating copper oxide layer was mechanically cleaned from the surface at the location where the sample was pressed by the copper ring which, in turn, was in electrical contact with the Wehnelt cylinder surface of the cathode assembly.

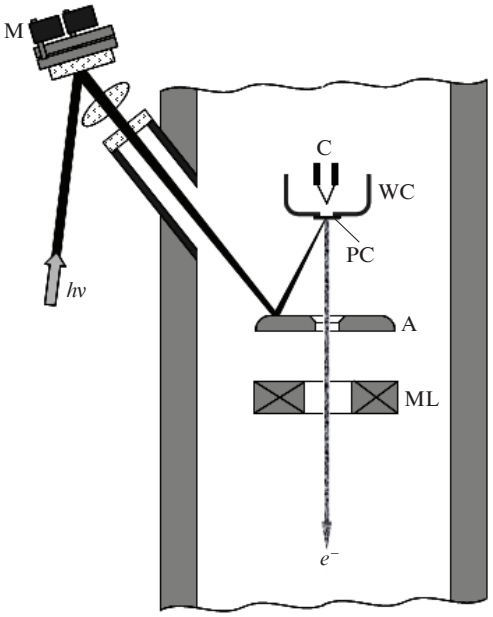

Figure 4. Scheme of the experiment: (C) cathode assembly; (WC) Wehnelt cylinder; (PC) photocathode based on the Cu_2O–Ag structure under study; (A) anode; (ML) microscope magnetic lens; (M) motorised precision mount of the folding mirror.

which made it possible to localise the emission of electrons on the photocathode surface. The emission of electrons from such a localised photoemission spot was conducted by superimposing the spot of focused laser radiation onto the photoemission spot. To facilitate the adjustment of laser radiation to the photoemission spot, a square grid of photoemission spots with a step of 120 μm along the axes and a total size of ~2 × 2 mm was formed on the photocathode surface (Fig. 2b).

To study the properties of the manufactured photocathode, an ultrafast transmission electron microscope was used, a detailed description of which is given in [13]. It represents an H-300 (Hitachi) modified commercial electron microscope with an accelerating voltage of 75 kV, in which a thermionic cathode is replaced by a photocathode, and an assembly is introduced for laser irradiation of a sample inside the microscope. The use of the same femtosecond laser with a beam splitted into two parts, between which an adjustable optical delay was introduced, for electron emission from the photocathode and for excitation of the sample under study made it possible to study in stroboscopic regime the dynamics of excitation and relaxation of the sample under investigation on a time scale up to 1 ns with a temporal resolution of few picoseconds.

The photocathode under study was placed on the outer surface of the Wehnelt cylinder of the microscope's cathode

Electrons emitted from the photocathode were accelerated to energy of 75 keV and, through the hole in the anode, entered the electron microscope column to form an electron beam using magnetic focusing systems. In our experiment, the microscope was switched to the 'diffraction' mode. In this regime, the microscope magnification is switched off, and the formed electron beam, after passing through the sample location area, is focused into a minimum spot on the surface of the vacuum-tight fibre-optic plate onto which a phosphor layer has been deposited. The phosphor layer was covered with a thin protective layer of aluminium, transparent to electrons with an energy of 75 keV. The electron beam image formed due to phosphor glow under the incident electron beam action was recorded in the photon counting regime using a C11440-22C digital camera (Hamamatsu) equipped with a Nikkor 24 (Nikon) lens. The effective number of pixels of the video camera's recording matrix was 2048 × 2048 with a pixel size of 6.5 × 6.5 μm. The pixel size of the recording system made it possible to observe the electron beam evolution in various parts of its image. In this case, the photoemission spot displacement caused by a small shift of the laser beam on the surface of the metal photocathode in the microscope, resulted in approximately the same displacements of the electron beam image on the video camera's recording matrix.

To initiate photoemission from the microscope cathode, we used in the experiment the fourth-harmonic radiation (263 nm) from the Antaus (Avesta-Project) femtosecond fibre laser with a pulse duration of ~300 fs and a maximum pulse repetition rate of 500 kHz. Using an optical shutter positioned at the fibre laser output, the pulse repetition rate could be widely varied from 500 kHz to 250 Hz. In our measurements, the laser pulse repetition rate and laser radiation power were selected in such a way that, in the course of signal accumulation on the video camera's recording matrix, the signal corresponding to the highest image brightness of the electron beam did not exceed the maximum range for the recording pixels of the matrix ($\sim 6.5 \times 10^4$ counts per pixel) and at the same time was large enough (over 2×10^4 counts), so that the shot noise impact on the measurement results could be neglected. In addition, the signal linearity was tested prior to measurements both as a function of the laser pulse repetition rate and the laser radiation power. The typical energy of the laser radiation pulse triggering photoemission in the course of measurements was in the range from 0.1 to 0.5 nJ.

Using a quartz lens, UV laser radiation was focused on the photocathode surface into a spot with a diameter of ~40 μm, which completely covered one of the photoemission spots on the photocathode surface. A square grid of photoemission spots with a distance of ~120 μm between them significantly facilitated the laser radiation tuning to the photoemission spot. The distance was much larger than the laser spot diameter, but smaller than the realignment region of the laser beam position on the cathode surface (~140 μm at the change level of 0.8), within which a slight reduction in the signal at the expense of receiving aperture of the microscope was observed. Preliminary alignment of the grid of photoemission spots on the photocathode relative to the central part of the microscope's cathode assembly was conducted in accordance with the position of an opening in the Wehnelt cylinder.

The laser beam scanning across the photocathode surface was conducted by tilting the mirror mounted on the alignment stage equipped with precision motorised movements along both alignment coordinates (see Fig. 4).

3. Results and discussion

To visually observe the localisation of electron photoemission on the photocathode surface under study, electron beam images were recorded in two regimes on the recording video camera of the electron microscope. In the first regime, laser radiation was adjusted to the photoemission spot on the photocathode surface in accordance with the maximum brightness of the electron beam image on the video camera, and the signal coming from the video camera's recording matrix was accumulated for a specified time interval (10 s). The image thus averaged over the accumulation time was stored in a computer. In the second regime, the beam image was obtained under the same conditions and at the same accumulation time as in the first regime, but with simultaneous automatic laser beam scanning over the photocathode surface under study in the direction (with intersection) of the photoemission spot. To do this, after adjusting the laser radiation to the photoemission spot, the laser beam was removed from the spot by about 70 μm and its automatic scanning over the photocathode surface in the direction of the photoemission spot was switched on.

The scanning speed was selected in such a way that, during the signal accumulation on the video camera, the laser beam was shifted by a distance of ~140 μm. To reduce the impact of neighbouring photoemission spots on the observed pattern, the laser beam scanning over the photocathode surface was performed over the diagonal of a square grid of photoemission spots (see Fig. 2b). For comparison, a similar electron beam image was obtained during scanning in the same range of laser radiation over the surface of a conventional photocathode in the form of a thin Ag film with no copper oxide layer.

It should be noted that the photoemission efficiency in using a sample with a photoemission spot under study was about an order of magnitude less than the photoemission efficiency for a sample in the form of an Ag film. This is explained by about seven-fold difference in the laser beam and photoemission spot areas, and also by the small losses associated with the presence of the Cu_2O film fragments on the photoemission surface, which, apparently, got there during the process of preparation (see Fig. 3a).

Figure 5 shows the electron beam image in using the Ag film as a photocathode with laser radiation scanning over the photocathode surface in the course of signal accumulation, and that of the Cu_2O–Ag structure with a photoemission spot with and without laser radiation scanning. It can be seen that, in the case of a photocathode in the form of the Ag film, there occurs expected image 'blurring' in the radiation scanning during the signal accumulation time. At the same time, in the case of laser beam scanning over the photocathode surface with the Cu_2O–Ag structure, the image 'blurring' is much smaller; it only slightly differs from that in the static image obtained for the same structure with no scanning.

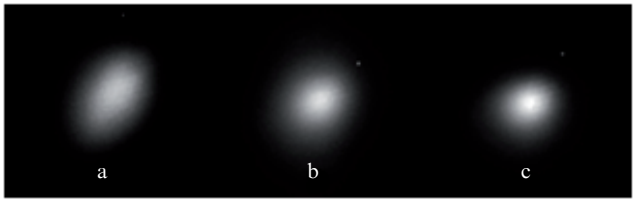

Figure 5. Electron beam images obtained using an Ag film as a photocathode with laser scanning over the photocathode surface during the signal accumulation time (a) and the Cu_2O – Ag structures with a photoemission spot during laser radiation scanning (b) and without scanning (c).

The images obtained qualitatively confirm that, in using the photocathode based on the Cu_2O–Ag structure, a 'binding' of photoelectron emission to the emission spot on the structure surface and its localisation occur in the course of laser radiation displacements from the emission spot.

In order to quantify the impact of the surface localisation of photoelectron emission in the electron microscope on the noise associated with spatial fluctuations of the laser radiation initiating photoemission, the fluctuations of the brightness-weighted 'centre of mass' (centroid) of the electron beam image were investigated in two cases: when using a conventional photocathode in the form of the Ag film, and also when using a photocathode in the form of the investigated Cu_2O–Ag structure with a photoemission spot. In both cases, a sequence of 100 images was recorded over a certain period of time (~10 min), with an accumulation time of 100 ms for

each image. The coordinates of the centroid, C_x and C_y, in the images obtained were calculated by standard formulas

$$C_x = \frac{\sum_{m,n} S_{m,n} n}{\sum_{m,n} S_{m,n}}, \quad C_y = \frac{\sum_{m,n} S_{m,n} m}{\sum_{m,n} S_{m,n}},$$

where n, m are the ordinal numbers of pixels in the columns and rows of the video camera's recording matrix; and $S_{m,n}$ is the signal magnitude in the pixel n, m.

Figure 6 shows the dependences of the position of the centroid of the electron beam image along one of the coordinates on the video camera's recording matrix, obtained for a sequence of 100 images with the use of the Ag film [curves (*1*) and (*2*), taken at different times] and the Cu_2O–Ag structures with a photoemission spot [curves (*3*) and (*4*)]. Similar results were obtained for the other coordinate. It follows from this figure that the centroid fluctuations in electron beam images in the case of using the Cu_2O–Ag structure are reduced as compared to relevant fluctuations in the case of the Ag film. Numerical calculations for each of the dependences presented in Fig. 6 result in the standard deviations of the image centroid, equal to 0.17, 0.19, 0.073, and 0.078 of pixel for curves (*1*–*4*), respectively.

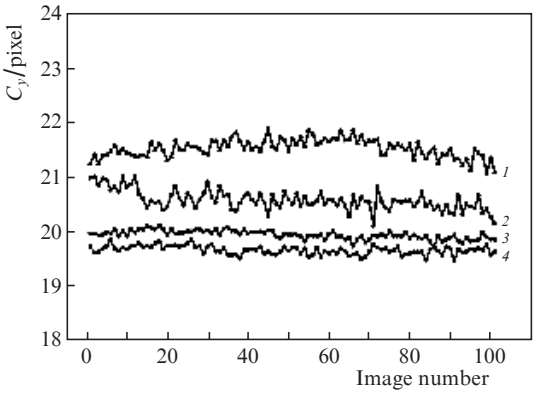

Figure 6. Fluctuations of the position of the centroid of the electron beam image along one of coordinates on the video camera's recording matrix, obtained for a sequence of 100 images with the use of an Ag film as a photocathode [curves (*1*, *2*) taken at different times] and a Cu_2O–Ag structure with a photoemission spot (*3*, *4*).

Comparison of these values shows that fluctuations decrease by about 2.2–2.6 times. This suggests that the spatial stability of the photoelectron beam increases with electron emission localisation on the cathode using the Cu_2O–Ag structure under study. It is also seen from Fig. 6 that slow variations of the image centroid contribute significantly to the dependences observed. The values characterising these slow variations, calculated as the dispersion magnitude from minimum to maximum value in the mean line of each of the dependences are 0.49, 0.56, 0.18, and 0.14 of pixel for curves (*1*–*4*), respectively. A significant decrease in these variations (by three to four times) with the localisation of electron emission on the photocathode surface suggests that these variations are apparently associated with a slow change in the laser beam position on the photocathode surface, presumably as a result of relatively slow local ambient temperature fluctuations, which lead to spatial instability of the laser beam.

It should be noted that the coordinate measurement error of the image centroid, associated with discreteness of the structure of the video camera's recording matrix, in the case when the diameter of electron beam image observed in the experiment is about 10 pixels, turns out much smaller (less than 0.01 of pixel [14]), and does not affect the measurement results.

In the light of the studies performed, it is of interest to use, as a photocathode, a structure with a photoemission spot of smaller diameter (of the order of several micrometers). This can result in a significant reduction in the fluctuation noises. Indeed, when a laser beam with inhomogeneous transverse energy distribution (e.g., Gaussian) is displaced relative to the photoemission spot, the electron emission efficiency is redistributed within the spot, which leads to a shift in the centroid of the electron beam in its cross-section. Obviously, this displacement cannot go beyond the emission spot, and therefore, as the photoemission spot diameter decreases, the laser beam fluctuations lead to smaller spatial fluctuations of the electron beam. It should be noted, however, that for small diameters of the photoemission spot compared to the laser beam diameter, residual photoemission from the photocathode region located around the photoemission spot can make a significant contribution to electron emission. In this case, provided the laser beam is displaced, the electron beam displacement is determined not only by the emission of electrons within the spot, but also by electrons emitted from the surface around the spot.

In order to estimate the contribution of this part of photoelectrons to the spatial position of the centroid of the total electron beam with respect to the contribution of the part of electrons emitted from the photoemission spot, we may assume that the former contribution is proportional to the ratio of the areas of laser and photoemission spots on the cathode and inversely proportional to the coefficient G of photoemission suppression by the Cu_2O layer. It is also assumed that the photoemission spot diameter is much smaller than the laser beam diameter on the photocathode surface, it is located at the laser beam centre, and the laser beam displacements relative to the photoemission spot are small (much smaller than the beam diameter). For example, for the laser beam diameter $D = 40$ μm, the photoemission spot diameter $d = 15$ μm, and the coefficient $G = 50$, this contribution is $(D/d)^2/G \approx 0.14$. This means that the centroid position for the electron beam emitted from the cathode surface is determined mainly by the part of electrons emitted from the photoemission spot. At the same time, at $D = 40$ μm, $d = 5$ μm and $G = 50$, this contribution constitutes ~1.3, i.e. in this case, the photocathode surface surrounding the photoemission spot makes a significant contribution to the electron beam formation, while the spatial fluctuations of the electron beam virtually repeat the spatial fluctuations of the laser beam. Therefore, in the case of a photocathode with a relatively small diameter of the photoemission spot, it is necessary to significantly (to the level of several hundred) increase the coefficient G of photoemission suppression on the photocathode surface outside the spot. Obviously, as the size of photoemission spot decreases, a fraction of radiation incident into this spot decreases, and, consequently, the laser radiation efficiency also decreases. Therefore, when reducing the photoemission spot diameter to several micrometers, it is advisable to proportionally reduce the laser beam diameter by focusing the radiation into a spot of smaller diameter (~10 μm). This obviously makes sense only if the spatial fluctuations of the

laser beam are smaller than its size on the photocathode surface. Reducing the laser beam diameter will not only increase the laser radiation efficiency, but also relax the requirements for the required value of the coefficient of photoemission suppression from the cathode outside the photoemission spot.

4. Conclusions

We have proposed a method for localisation of photoelectron emission, based on the formation of photoemission spots on the photocathode surface by suppression of photoemission of electrons from the photocathode surface outside these spots. To develop such a photocathode, a structure of thin Cu_2O and Ag films was used, on which, by means of laser processing technique, a grid of photoemission spots with a diameter of ~15 μm was formed. Studies have shown that the use of such a photocathode in an ultrafast electron microscope results in two- or three-fold reduction of the noises associated with spatial fluctuations of laser radiation initiating photoemission of electrons. In order to further reduce these noises, it is of interest to reduce the photoemission spots to a size of a few microns while simultaneously increasing the coefficient of photoemission suppression from the photocathode surface outside the emission spots.

It should also be noted that the method proposed for localisation of photoelectron emission on the photocathode surface can be used not only for film-type, but also for massive photocathodes. In addition, this method can be used not only in the case of direct incidence of laser radiation on the photocathode surface, but also in the reverse incidence (in transmission regime). These capabilities significantly increase the versatility of employing this method for photoelectron emission localisation.

Acknowledgements. Experiments on photoelectron emission were performed using the Unique Scientific Setup 'Multipurpose femtosecond laser-diagnostic spectrometry complex' at the Institute of Spectroscopy, Russian Academy of Sciences. The nanostructure for photoelectron emission localisation was manufactured at the Laboratory of Gas Lasers of the Department of Quantum Radiophysics, P.N. Lebedev Physical Institute.

S.V.A. and E.A.R. are thankful to V.O. Kompanets, B.N. Mironov, and S.V. Chekalin, and P.A.D. and S.I.K. are thankful to A.A. Rudenko and A. A. Ionin for their assistance in conducting experiments.

This work was supported by the Ministry of Education and Science of the Russian Federation (Project No. FMEFI61316X0054).

References

1. Ishchenko A.A., Aseev S.A., Bagratashvili V.N., Panchenko V.Ya., Ryabov E.A. *Usp. Fiz. Nauk*, **184**, 681 (2014).
2. Zewail A.H., Thomas J.M. *4D electron microscopy: imaging in space and time* (London, UK: Imperial College Press, 2009; Dolgoprudny: Intellect, 2013).
3. Baskin J.S., Zewail A.H. *Compt. Rend. Phys*., **15**, 176 (2014).
4. Miller R.J.D. *Ann. Rev. Phys. Chem*., **65**, 583 (2014).
5. Barwick B., Corder C., Strohaber J., Chandler-Smith N., Uiterwaal C., Batelaan H. *New J. Phys*., **9**, 142 (2007).
6. Casandruc A., Kassier G., Zia H., Bücker R., Miller R.J.D. *J. Vac. Sci. Technol. B*, **33**, 03C101 (2015).
7. Storeck G., Vogelgesang S., Sivis M., Schäfer S., Ropers C. *Structural Dynamics*, **4**, 044024 (2017).
8. Hoffrogge J., Stein J.P., Krüger M., Förster M., Hammer J., Ehberger D., Baum P., Hommelhoff P. *J. Appl. Phys*., **115**, 094506 (2014).
9. Plemmons D.A., Flannigan D.J. *Chem. Phys. Lett*., **683**, 186 (2017).
10. Meyer B.K., Polity A., Reppin D., Becker M., Hering P., Klar P.J., Sander Th., Reindl C., Benz J., Eickhoff M., Heiliger C., Heinemann M., Bläsing J., Krost A., Shokovets S., Müller C., Ronning C. *Phys. Status Solidi B*, **249**, 1487 (2012).
11. Danilov P.A., Zayarnyi D.A., Ionin A.A., Kudryashov S.I., Litovko E.P., Mel'nik N.N., Rudenko A.A., Saraeva I.N., Umanskaya S.F., Khmelnitskii R.A. *Pis'ma Zh. Eksp. Teor. Fiz*., **105**, 693 (2017).
12. Danilov P.A., Zayarnyi D.A., Kudryashov S.I., Ionin A.A., Nguyen Ch.T.H., Rudenko A.A., Saraeva I.N., Kuchmizhak A.A., Vitrik O.B., Kulchin Yu.N. *Pis'ma Zh. Eksp. Teor. Fiz*., **103**, 617 (2016).
13. Andreev S.V., Aseev S.A., Bagratashvili V.N., Vorobyev N.S., Ishchenko A.A., Kompanets V.O., Malinovskiy A.L., Mironov B.N., Timofeev A.A., Chekalin S.V., Shashkov E.V., Ryabov E.A. *Quantum Electron*., **47**, 116 (2017) [*Kvantovaya Elektron*., **47**, 116 (2017)].
14. Starosotnikov N.O., Fedortsev R.V. *Nauka i Tekhnika*, (5), 71 (2015).